Quantum Electronics **51** (10) 878–885 (2021)

https://doi.org/10.1070/QEL17623

Application of liquid low-temperature cooling in a multi-disk ytterbium laser head under conditions of multi-joule pumping at a high pulse repetition rate

M.R. Volkov, I.B. Mukhin

Abstract. **We have investigated the possibility of low-temperature liquid cooling of a multi-disk laser head, as well as the main advantages of this approach. The active zone of the laser head was modelled: the temperature, coolant velocity, inversion, gain, stored energy in the active medium, and thermally induced phase distortions were calculated. It was shown that such cooling can be accomplished with ethyl alcohol; there also are more preferred liquids, which are more difficult in use. The optimal parameters of the active zone were found for using pump pulses with an energy of several J. A significant increase in the gain and stored energy were shown upon cooling from 300 to 200 K, as was a decrease in thermally induced phase distortions.**

Keywords: *liquid low-temperature cooling, ethanol, multi-disk ytterbium laser head, thermally induced phase distortions, cooling efficiency.*

1. Introduction

Amplification of laser pulses to high energies calls for the use of large-volume active elements, in which the role of amplified spontaneous emission increases and there occurs self-focusing as well as distortion of the phase and time profiles. Operation of the amplifier at a high pulse repetition rate (with a high average output power) implies the necessity for efficient heat removal from the active zone. There are a number of laser designs [1–6] based on active elements in the form of slabs (disks), which are designed to achieve these goals and feature the cooling of active elements from the optical surfaces. When using active elements in the form of slabs, their large aperture is an advantage from the point of view of radiation resistance, at the same time allowing a high thermal power to be dissipated. However, in this case the radiation inevitably passes through the coolant, which may introduce additional phase distortions of the radiation. In this regard, the key issue is the choice of the coolant and the cooling regime. The use of cryogenically cooled gaseous helium [1] introduces minimal phase distortions and makes it possible to realise the advantages of ytterbium media at cryogenic temperatures [7]. However, due to its very low volume heat capacity, the time-averaged power density is significantly limited even at increased coolant pressure. Cooling with heavy (deuterated) water [2] is efficient and simple to implement, but the minimum achievable temperature is limited by the freezing point of water, which does not permit using the advantages associated with cooling to cryogenic temperatures.

This paper analyses the possibility of applying liquid cooling using a refrigerant with a freezing point of about –100 °C and below. In doing this, it is possible to partially combine the advantages of liquid and cryogenic cooling. Note that today there are commercially available refrigeration units achieving temperatures down to –100 °C and having a relatively high heat removal capacity [8, 9]. Such systems are much cheaper and easier to operate than cryogenic helium systems, which allows them to be effectively used for a wide range of scientific and technological problems, including laser engineering. As a refrigerant, it is possible to use various alcohols (we have considered the possibility of using ethyl alcohol). To reduce radiation losses, various antifreezes, acetone, 'gasoline', etc., can be used as a coolant. In this study, we consider longitudinal pumping by the homogenised radiation of diode assemblies. This approach makes it possible to achieve a peak pump power of tens of kilowatts and provides the best overlap between the pump beam and the laser beam, in contrast to configurations with lateral radiation pumping [5, 6].

2. Measurement of radiation absorption in a number of liquids

When the optical faces of the active element are used simultaneously as heat sinks, the radiation inevitably passes through the coolant. Therefore, it becomes important not only to ensure a laminar flow of the liquid, but also to minimise the possible absorption of radiation in it. The possible losses of radiation in the coolant will lead to a decrease in optical efficiency, additional heating, and phase distortions. In this connection, we analysed the magnitude of linear losses in various cooling media, and also carried out additional measurements. The measurement of absorption in a number of liquids was carried out according to the configuration depicted in Fig. 1.

The source of broadband radiation is a halogen lamp, the radiation of which is directed into a liquid-filled cuvette. At the bottom of the cuvette there is a mirror with a multilayer dielectric coating. The reflection loss from the mirror in air is less than 10^{-3} in the wavelength range 920–1100 nm. The beam reflected from the mirror enters the optical fibre, which serves as the input port of the spectrometer. The spectrum of

M.R. Volkov, I.B. Mukhin Institute of Applied Physics, Russian Academy of Sciences, ul. Ulyanova 46, 603950 Nizhny Novgorod, Russia; e-mail: bearuck@mail.ru

Received 4 April 2021; revision received 11 August 2021
Kvantovaya Elektronika **51** (10) 878–885 (2021)
Translated by E.N. Ragozin

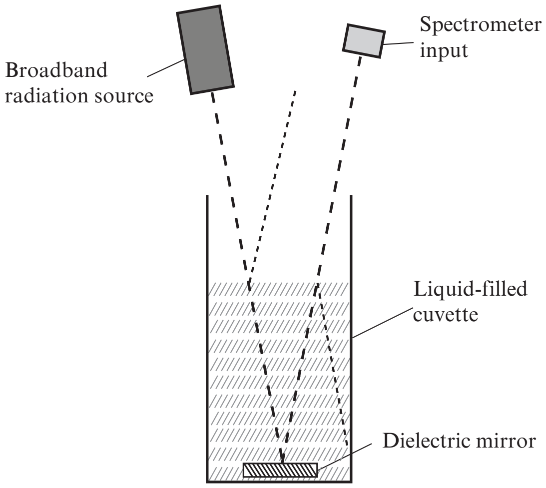

Figure 1. Scheme for measuring the absorption of radiation in a liquid.

radiation coming from the cuvette is recorded at several different heights of the liquid column. By comparing the resultant spectra, it is easy to obtain the linear loss coefficient. This procedure was performed for several liquids; the results are shown in Fig. 2. The literature contains data on absorption in light and heavy water [2]; the results presented in our work are in good agreement with them.

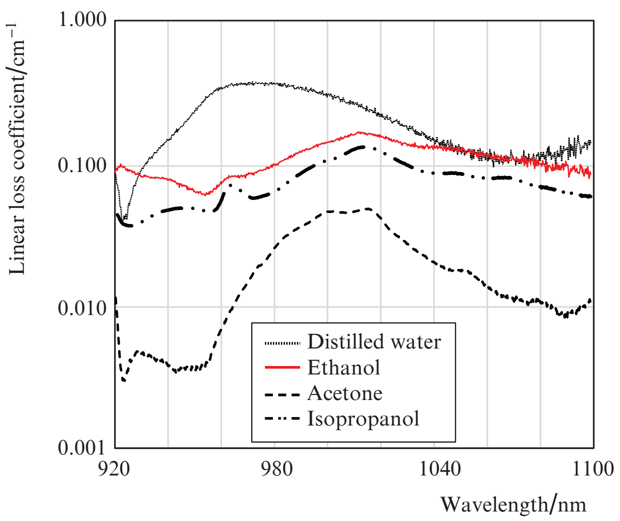

Figure 2. Linear loss spectra in liquids.

As follows from Fig. 2, when ethanol is used as a cooling liquid, the radiation loss at a wavelength of 1030 nm is about 14% for a layer thickness of 1 cm. As shown below, such absorption is insignificant both for heat sources and for signal amplification.

3. Simulation of thermal distortion and amplification in a multi-disk laser head

We take a closer look at the geometry of the multi-disk laser head. The active zone of the laser (laser head, Fig. 3) is a cuvette (vessel) with a cooling liquid, into which solid-state active elements in the form of plane-parallel slabs are immersed. The slab thicknesses are several times smaller than their transverse size. The coolant is pumped through the gaps (channels) between the slabs, and the fluid flows can be directed either in one direction or in the opposite direction with respect to the adjacent channel. The thicknesses of all gaps (channels) are the same, but the slab thicknesses are varied. The active zone is limited by optical windows, which transmit the pump and signal radiation.

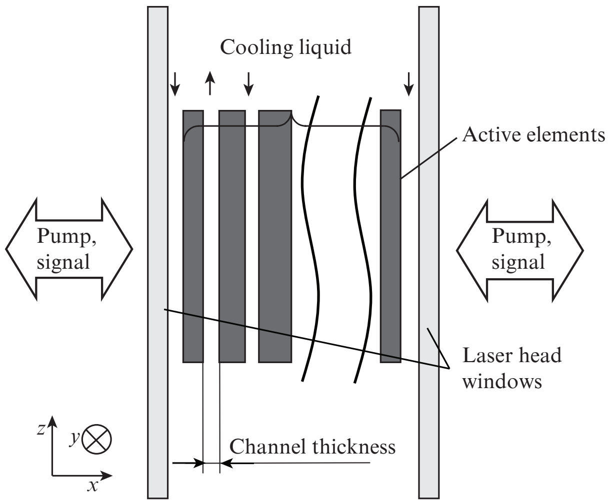

Figure 3. Schematic of a laser head. The light aperture of the laser head is square.

It is assumed that the laser head operates in the regime of pulsed pumping at a wavelength of 940 nm for a pulse repetition rate above 20 Hz. In the pumping by 940 nm radiation, the quantum defect is the main mechanism of heat release; in addition, there are linear radiation losses in the liquid (see Fig. 2), which are an additional source of heating. The Yb : YAG material (unlike, for example, Nd : YAG) is characterised by the fact that only the quantum defect makes a major contribution to heat release both in the case of spontaneous luminescence of stored energy and in the case of signal-induced energy extraction [10]. The quantum defect is 8.7% for amplification with saturation and 6.5% for free luminescence. The simulation was carried out for the quantum defect of 8.7% (i.e., the worst version). The contribution of heat sources would therefore be expected to be slightly less than in the numerical simulation performed.

The temperature distribution was calculated by jointly solving the thermal conductivity and Navier–Stokes stationary equations with given heat sources for a given pressure gradient in the coolant:

$$-\nabla(k\nabla T) = Q - \rho C(\boldsymbol{u}\nabla T), \tag{1}$$

$$\rho(\boldsymbol{u}\nabla)\boldsymbol{u} = -\nabla p + \eta\Delta\boldsymbol{u} + \boldsymbol{f}. \tag{2}$$

Here k is the thermal conductivity coefficient; T is the temperature field depending on three spatial coordinates; Q is bulk density of heat sources; ρ is the density of the medium; C is the heat capacity of the medium; $\boldsymbol{u}$ is the velocity field; p is the pressure; η is the dynamic viscosity of the fluid; and

f is the field of mass forces. For the equation of thermal conductivity, we used the boundary conditions of zero heat flux at the side surface of the active disks and the conditions of temperature continuity at the faces of the disks. Note that taking into account the finite heat transfer coefficient [5 W (K cm^2)$^{-1}$] leads to a change in the maximum temperature of active disks by no more than 7%, which is why we considered simpler boundary conditions of temperature continuity. The choice of stationary equations in this case is justified, since in the geometry shown in Fig. 3, the characteristic decay time of the lowest mode of the temperature field is 0.3 s, which is significantly longer than the time interval between pump pulses. The decay time of the higher modes of the temperature field is comparable with (and even shorter than) the interval between pump pulses, but these modes are not important from the viewpoint of radiation distortions.

The applicability of the stationary model is clearly illustrated in Fig. 4a, which shows the calculated time dependence of the maximum temperature in the active zone at a pump pulse repetition rate of 100 Hz. One can see that the temperature variation in the interval between pump pulses is less than 1 K, while the maximum temperature is 20 K higher than the coolant temperature. The fraction of radiation converted to heat in the active medium is equal to the Stokes shift (quantum defect) between the pump and laser signal photons. The active medium is yttrium aluminium garnet doped with ytterbium (Yb: YAG). The laser signal has a wavelength of 1030 nm, and the pump wavelength is 940 nm. The power of heat sources in the cooling liquid is determined by the absorption coefficient of the pump radiation. These coefficients were measured in a number of liquids (see Fig. 2). In this work, we present calculations for ethanol as a cooling liquid; the pump loss is taken to be 0.08 cm^{-1}.

It is well known that the dynamic viscosity of ethanol increases 15-fold with a decrease in temperature from +20 to –80 °C [11]. The dependence borrowed from Ref. [11] was approximated by the function

$$\eta = \frac{3.5 \times 10^{16}}{T^8} + \frac{10^4}{T^3}, \quad (3)$$

where η is the dynamic viscosity in Pa s and T is the temperature on the Kelvin scale. When the active medium is cooled by a liquid, as shown in Fig. 3, the latter introduces phase distortions into the signal radiation. An important point is the choice of the cooling flow velocity, since a turbulent flow gives rise to small-scale nonuniformities of the temperature, refractive index and, as a consequence, phase distortions of the signal, which randomly depend on time and coordinates [12]. The fluid flow in a plane-parallel channel is characterised by the Reynolds number:

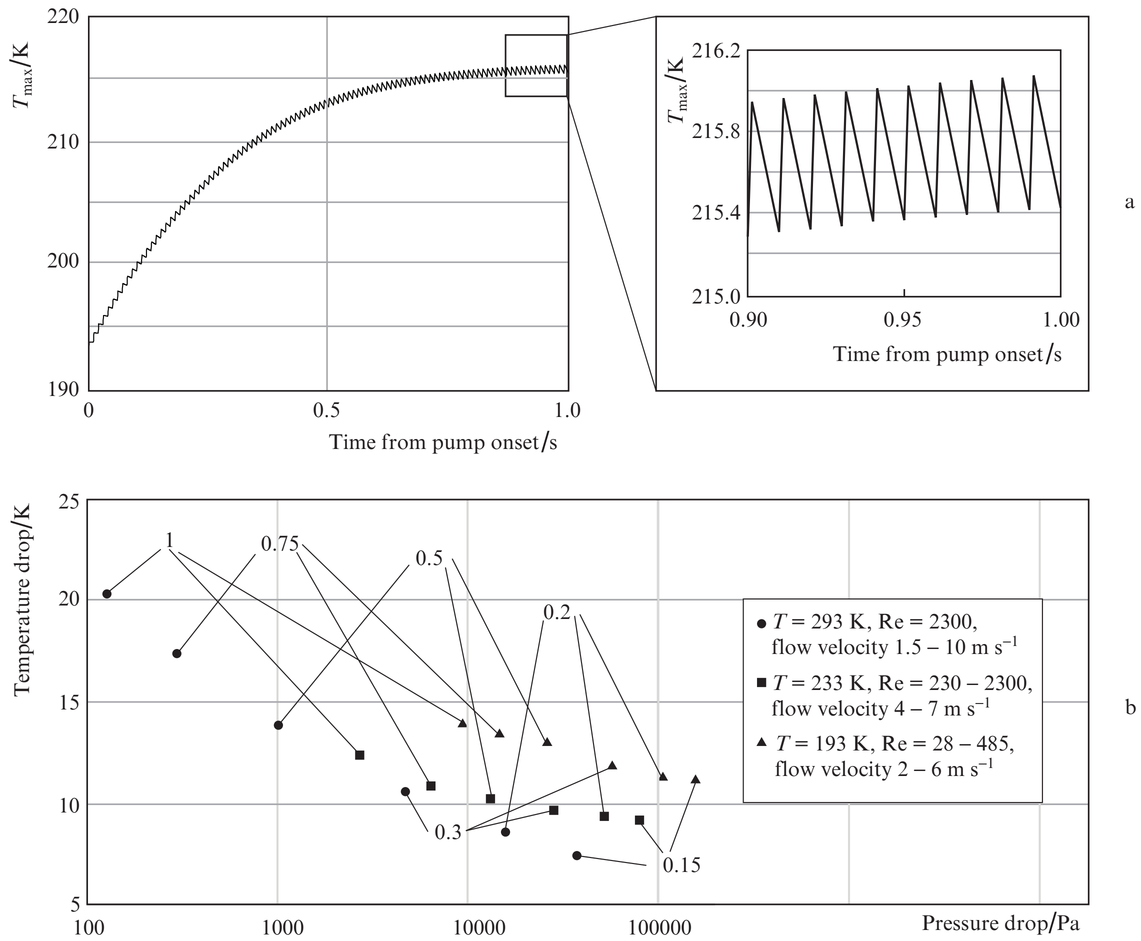

Figure 4. Time dependence of the maximum temperature in the active zone (6 slabs 1 mm thick, the channel thickness is 0.5 mm, the pressure drop is 10 kPa); (b) cooling efficiency versus coolant temperature, pressure drop and channel thickness. Channel thickness in millimetres is indicated in the figure.

$$\mathrm{Re} = 2uh\rho/\eta, \tag{4}$$

where u is the flow speed; h is the channel thickness; and ρ is the liquid density. The condition of flow laminarity,

$$\mathrm{Re} < 2300, \tag{5}$$

imposes an upper limit on the flow velocity. On the other hand, for a given channel thickness and pressure gradient, the flow velocity field is determined from the stationary Navier–Stokes equation (2):

$$\boldsymbol{u} = z_0 u_{\max} 4x(x-h)/h^2, \tag{6}$$

$$u_{\max} = \frac{Ph^2}{8l\eta}. \tag{7}$$

Here $u_{\max}$ is the maximum flow velocity in a plane-parallel channel; l is the channel length; and P is the differential pressure provided by the pump. It is assumed that the flow is laminar, the channel of thickness h is parallel to the yz plane, and x is the coordinate along the normal to this plane. By substituting expression (7) into expressions (4), (5), it is possible to estimate the maximum allowable pressure drop for a given fluid viscosity, channel thickness and flow laminarity condition. A more accurate calculation of the velocity field is performed numerically, taking into account the temperature dependence of the viscosity in accordance with formula (3).

Thermally induced phase distortions were calculated using the thin lens formula

$$\Delta\Phi(y,z) = \int_{x_1}^{x_2} T(x,y,z)\frac{\mathrm{d}n(x)}{\mathrm{d}T}\mathrm{d}x. \tag{8}$$

Here $\Delta\Phi(y,z)$ is the change in the optical path, depending on the coordinates y, z of the point on the light aperture (integration is carried out along the beam path within the laser head); $T(x,y,z)$ is the temperature field in the laser head; and $\mathrm{d}n(x)/\mathrm{d}T$ is the thermooptical coefficient [11, 13].

The calculation of the inversion in the active medium (Yb:YAG) was carried out using the balance equations:

$$\frac{\mathrm{d}n_{\mathrm{up}}}{\mathrm{d}t} = -\frac{n_{\mathrm{up}}}{\tau} + \frac{I_{\mathrm{p}\Sigma}}{h\nu_{\mathrm{p}}}[\sigma_{\mathrm{abs}}(\lambda_{\mathrm{p}})n_{\mathrm{down}}q_{\mathrm{p}} - \sigma_{\mathrm{em}}(\lambda_{\mathrm{p}})n_{\mathrm{up}}], \tag{9}$$

$$\frac{\mathrm{d}I_{p1+}}{\mathrm{d}x} = I_{\mathrm{p}}N_{\mathrm{dop}}[-\sigma_{\mathrm{abs}}(\lambda_{\mathrm{p}})n_{\mathrm{down}} + \sigma_{\mathrm{em}}(\lambda_{\mathrm{p}})n_{\mathrm{up}}], \tag{10}$$

$$n_{\mathrm{down}} + n_{\mathrm{up}} = 1, \tag{11}$$

where n_{up}, n_{down} are the relative populations of the upper and lower multiplets in the trivalent ytterbium ion [14]; x is the coordinate along the direction of pump and signal propagation; τ is the lifetime of the upper laser level; $I_{\mathrm{p}\Sigma}$ is the total intensity of pump radiation, taking into account all passes; $I_{\mathrm{p1+}}$ is the intensity of the pump wave travelling only in the direction of the x axis during the first pass through the active zone [valid for an oppositely travelling wave is an equation similar to Eqn (10) with the opposite sign in the right side]; $h\nu_{\mathrm{p}}$ is the pump photon energy; $\sigma_{\mathrm{abs}}(\lambda)$ and $\sigma_{\mathrm{em}}(\lambda)$ are the cross sections of absorption and amplification at the wavelength λ; λ_{p} is the pump wavelength; and N_{dop} is the volume density of the Yb^{3+} ion. In Eqns (9) and (10), the cross sections σ_{abs}, σ_{em} depend on the temperature [7], which, in turn, depends on three spatial coordinates according to the numerical solution of the heat conduction equation. The density of the activator ion is assumed to be constant in the solid and equal to zero in the coolant. Equations (9)–(11) are solved with respect to the variables n_{up}, n_{down}, and I_{p}, which depend on three spatial coordinates and time. The solution is performed on a time interval corresponding to the duration of the pump pulse. The initial conditions are imposed on the population of the multiplets, and the boundary conditions are imposed on the pump radiation intensity:

$$n_{\mathrm{up}}(x, y, z, t = 0) = 0, \tag{12}$$

$$I_{\mathrm{p1+}}(x = 0, y, z, t) = I_{\mathrm{in}}(x = 0, y, z),$$

$$I_{\mathrm{p1-}}(x = x_{\max}, y, z, t) = I_{\mathrm{in}}(x = 0, y, z),$$

$$I_{\mathrm{p2-}}(x = x_{\max}, y, z, t) = I_{\mathrm{p1+}}(x = x_{\max}, y, z, t),$$

$$I_{\mathrm{p2+}}(x = 0, y, z, t) = I_{\mathrm{p1-}}(x = 0, y, z, t). \tag{13}$$

As a result of solving Eqns (9)–(11) with conditions (12), (13), we obtain the population distribution of the upper laser level n_{up}, whence one can calculate the distribution of the stored energy and the small-signal gain for a known cross section of the laser transition.

4. Influence of cooling characteristics on the temperature of the active medium

This work was performed with the aim of future practical application of the simulations presented in it. The choice of ethanol as a coolant is due to its low freezing point (159 K), a relatively low volatility (vapour pressure) at 300 K, and ease of handling. The calculation and optimisation of the parameters of the laser head were carried out for pump pulses at a wavelength of 940 nm with an energy of 4 J and a duration of 1 ms. A preliminary calculation based on Eqn (9) suggests that a significant (5-fold) excess of the pump threshold is achieved in a Yb:YAG medium when the pump spot diameter is 6 mm. At the same time, there is still no significant saturation of the medium, and so all further calculations were carried out for this diameter. The optical aperture of the active zone was assumed to be square with a side of 1 cm. Based on the heat conduction and Navier–Stokes equations, the temperature fields were calculated at different initial coolant temperatures, pressure drops, and channel thicknesses. A typical temperature distribution is shown in Fig. 5.

Our simulation suggests that the main temperature drop occurs in the coolant layer adjacent to the solid active medium. The temperature drop in the solid medium with a thickness of less than 2 mm is insignificant (less than 10%). The key parameters affecting the cooling efficiency are the channel thickness and coolant flow rate. One of the restrictions imposed on these parameters is indicated in formulae (4), (5). Another natural limitation arises from the heating of the

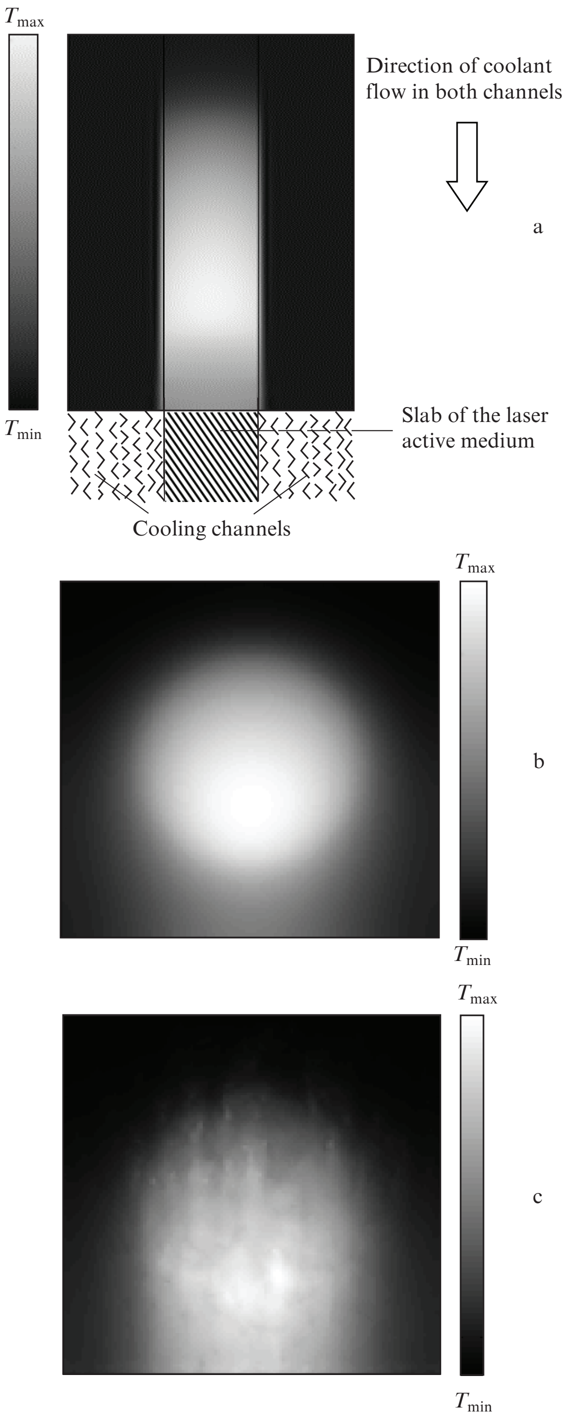

Figure 5. Calculated temperature distribution in one slab of the active medium and adjacent cooling channels: (a) two-dimensional section by a plane parallel to the coolant flow and perpendicular to the plane of the slabs; (b, c) two-dimensional section parallel to the slabs (b) in the solid and (c) in the liquid.

coolant as a result of the work of viscous forces in the cooling channels, pump, pipelines, etc. It is reasonable to assume that the power of viscous forces in the laser active zone should not exceed 10% of the thermal pump power. Another limitation is due to signal and pump loss in the cooling liquid. Assuming that the signal loss should not exceed 10%–15% in one pass through the laser head and the linear loss coefficient in the liquid (ethanol) is 0.15 cm^{-1} (see Fig. 2), the total channel thickness should not exceed 1 cm. Taking these limitations into account, we calculated the temperature fields in the laser head. The difference between the maximum and minimum temperatures (temperature difference) in the cuvette, which characterises the efficiency of heat removal, is shown in Fig. 4b. In this simulation, the average pump power is 400 W (approximately corresponds to pulses with an energy of 4 J at a repetition rate of 100 Hz), and it is evenly distributed over 10 slabs of the active medium.

The calculations took into account that the minimum channel thickness (0.1 mm) is limited by the manufacturing accuracy of such a laser head, as well as by the excessive pressure of the coolant, which requires special fittings. One can see from Fig. 4b that the cooling efficiency increases with a decrease in the thickness of the channels (and with an increase in pressure) at any temperature of the coolant. At lower initial coolant temperature, the temperature difference inside the laser cuvette is slightly higher due to greater viscosity of the coolant and lower cooling efficiency. However, this temperature increase is negligible compared to absolute temperature drop.

The results presented in Fig. 6 suggest that the pump absorption in the coolant has no noticeable effect on the heating of the laser head when ethanol is used as a cooling liquid. Under these conditions, the temperature difference increases linearly with increasing power at a constant flow rate of the coolant. The radiation absorption losses are close to the Fresnel losses at antireflection coatings, and the heat release associated with this absorption hardly affects the temperatures inside the active disks. The choice of the optimal number of slabs is a trade-off between the radiation loss and the required cooling efficiency, as well as the complexity of the laser head fabrication.

For further calculations of phase distortions and gain, it is necessary to select specific parameters of the active zone. It was assumed that the number of slabs is 6, the thickness of the slabs is 1 mm, the doping is 2%, the thickness of the channels is 0.5 mm, and the Reynolds number is 75. With an optical aperture of 1 × 1 cm and an initial coolant temperature of 193 K, the pressure drop over the channel length is 11 kPa, and the coolant flow rate is 2.6 L min^{-1}.

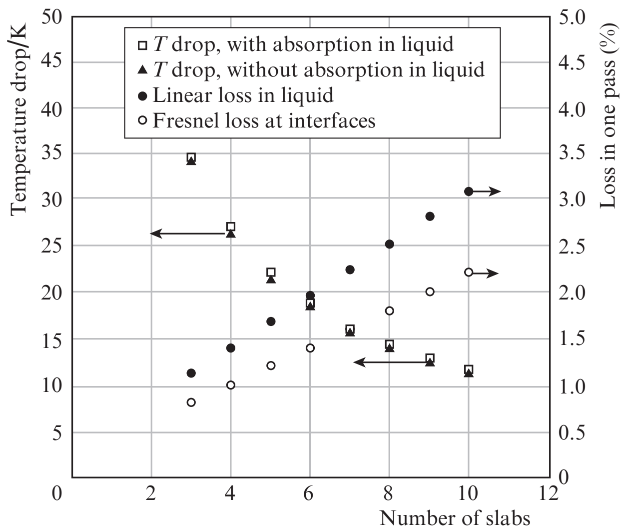

Figure 6. Cooling efficiency and radiation loss in relation to the number of slabs. Coolant temperature, 193 K; channel thickness, 0.2 mm; Reynolds number, 44; pressure drop, 106 kPa.

5. Phase distortions in the laser head geometry under consideration

Radiation distortion is one of the determining factors limiting the average power of solid-state lasers. A significant thermal lens and thermal wedge complicate the optical configuration of the amplifier, especially in the multi-pass case. Aberrations of the phase profile of the radiation lead to energy losses in the fundamental (required) transverse radiation mode.

As can be seen from Fig. 7, with a decrease in the coolant temperature from 293 to 193 K, the total magnitude of phase distortions changes slightly, since a decrease in dn/dT in the solid is partially offset by a slight deterioration in the cooling efficiency (see Fig. 4b). The thermally induced phase wedge in the described geometry arises due to the asymmetry of the coolant flow. This can be avoided by using opposite flows in adjacent channels. Calculation of the thermal problem suggests that the temperature difference in the two cases (flow in one direction and with a counterflow in adjacent channels) differs insignificantly (1.5%), but the change in the optical path becomes symmetric relative to the horizontal plane. Interestingly, when cooling with counterflows is realised, phase aberrations are significantly reduced (Fig. 8). The main quantitative results are summarised in Table 1.

The effect of thermally induced phase distortions on a laser beam involves, among other things, an increase in its spatial divergence. To assess this effect, the beam quality parameter M^2 was simulated in two cases: at coolant temperatures of 293 and 193 K, with a counterflow, at an average pump power of 400 W. A Gaussian beam with a diameter equal, at the 1/e^2 level, to 0.75 of the pump beam diameter was directed into the laser head. After one pass through the laser head, the parameter M^2 rises to 1.86 at a coolant temperature of 193 K and to 2.5 at a coolant temperature of 293 K, which is indicative of a significant advantage of the low-temperature cooling.

Note that the absorption of pump radiation in the liquid (see Fig. 6) has an insignificant effect on heating (less than one degree). Nevertheless, its contribution to phase distortions (Table 1, Fig. 7) is quite significant and amounts to about 15% due to the significantly higher dn/dT coefficient in the liquid.

6. Stored energy and small-signal gain

An important feature of ytterbium media is a significant improvement in their laser characteristics with decreasing temperature [7]. The amplification cross section increases significantly for a relatively constant lifetime of the upper laser level. The lower laser level is depopulated, and the scheme of energy levels goes from a quasi-three-level scheme to a four-level one. Based on Eqns (9)–(11) with a known distribution of temperatures and transition cross sections, we calculated the population of the upper laser level. Using the resultant population distribution, we calculated the stored energy and the small-signal gain at a wavelength of 1030 nm in two passes through the active zone. The transverse distribution of the gain without including the signal loss (see Fig. 6) is shown in Fig. 9. As the calculations show, a significant gain is achieved in this geometry (on average, more than 15-fold), and the stored energy is 2 J (Fig. 10) for pump pulses with a duration

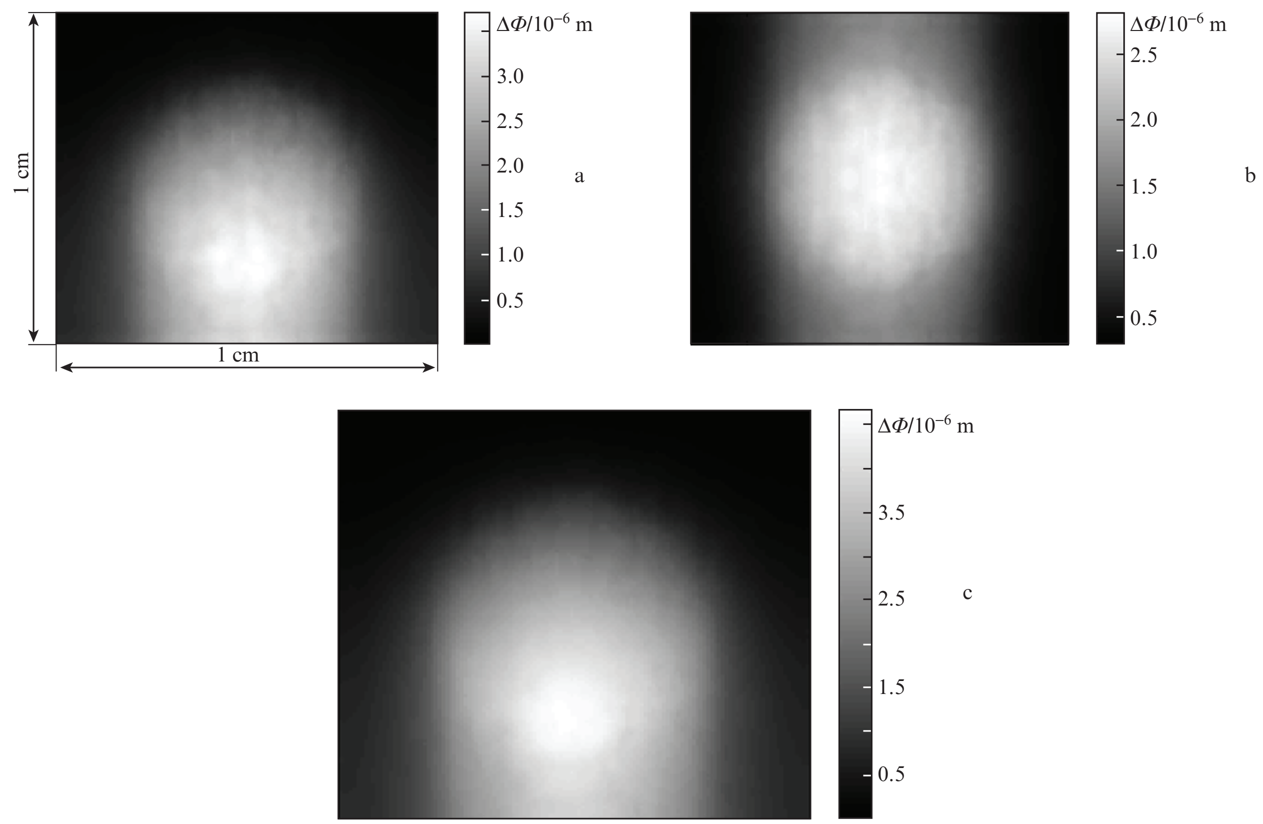

Figure 7. Phase distortions in the xy plane in a laser head in one pass at a coolant temperature of 193 K (a) for a one-way flow and (b) with a counter-flow as well as (c) at 293 K for a one-way flow.

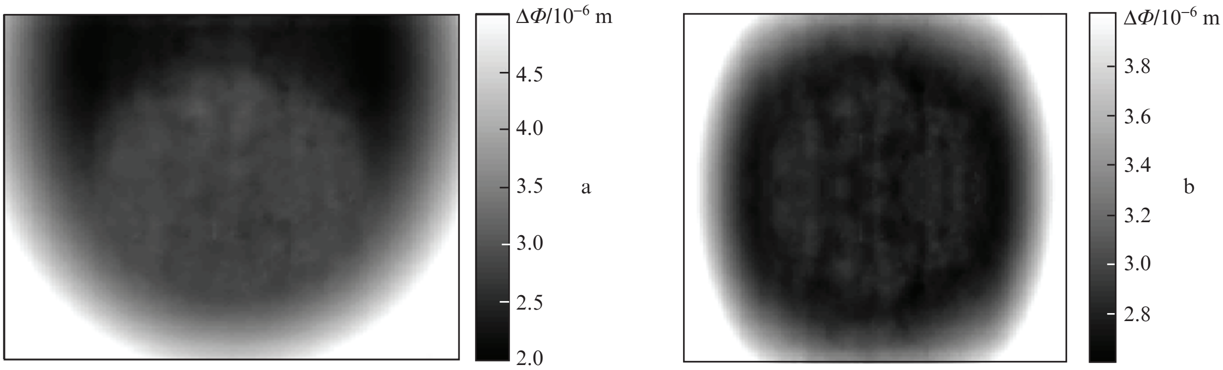

Figure 8. Phase distortions in the xy plane minus the thermal wedge and the parabolic component during cooling (a) with a flow in one direction and (b) with a counterflow.

Table 1. Linear and parabolic components of phase distortions in a laser head after one pass with the inclusion of absorption in the liquid (the flow is directed in one direction)*.

Distortion type	Active slab contribution		Coolant contribution		Total distortion	
	293 K	193 K	293 K	193 K	293 K	193 K
Thermal lens power, 1/m (vertical plane)	8.80 E-02	5.64 E-02	9.63 E-02	8.68 E-02	1.84 E-01	1.43 E-01
Optical wedge, rad (vertical plane)	−9.69 E-05	−6.00 E-05	−5.64 E-04	−4.44 E-04	−6.60 E-04	−5.04 E-04
Thermal lens power, 1/m (horizontal plane)	1.14 E-01	7.39 E-02	3.10 E-01	2.63 E-01	4.24 E-01	3.37 E-01

*In the case of counterflow, the powers of the lenses remain unchanged, the vertical wedge is zero.

of 1 ms, which corresponds to 4 J of energy. The effect of amplified spontaneous emission (ASE), which was not included in the simulations, will, of course, lead to a decrease in both the gain and the stored energy. Nevertheless, the effect of the ASE influence will be smaller than in active elements in the form of an active mirror or in a multi-disk laser head with helium vapour cooling, since the difference in the refractive index between the active medium and the coolant is smaller than between the active medium and the air (or helium). As a result, spontaneous emission is not 'blocked' by the angle of total internal reflection inside the inverted-population region. The simulation results for a shorter pump pulse duration are shown in Fig. 10. It follows from the simulation that the threshold pump energy density is significantly exceeded already for a pump pulse duration of 0.25 ms, which corresponds to an energy of 1 J, since an amplification by a factor of 2.6 is observed. Similar simulations at room temperature (293 K) and a pump pulse duration of 1 ms suggest that the stored energy is 1.5 J and the amplification is 3, which indicates the advantage of the outlined concept of liquid cooling of the active medium to a reduced temperature.

Figures 11 and 12 depict the results of calculating the gain and thermal effects in relation to the pump pulse repetition rate when using low-temperature cooling. One can see that an increase in the average power does indeed lead to some deterioration in the basic characteristics. However, in the frequency range under consideration, the decrease in the gain and the increase in the power of the thermal lens can be considered moderate. A more important limitation to average power is the refrigeration efficiency of a refrigeration unit, which in commercial units is limited to a few hundred watts at refrigeration temperatures below −50 °C.

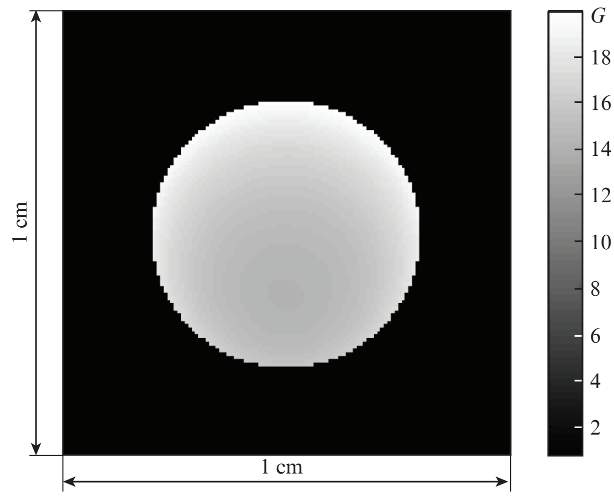

Figure 9. Small-signal gain (G) distribution in the xy plane for two passes through the laser head. Peak pump power, 4 kW; pulse duration, 1 ms; repetition rate, 100 Hz; coolant temperature, 193 K; channel thickness, 0.5 mm; Reynolds number, 75.

7. Conclusions

The paper proposes an original concept of a multi-disk amplifier module with active elements directly cooled by a low-temperature liquid refrigerant through optical surfaces. A numerical model has been developed for calculating thermal effects and the gain in the proposed geometry of the active medium. The possibility of using alcohols for cooling is analysed. We have estimated the geometric parameters of the active zone of

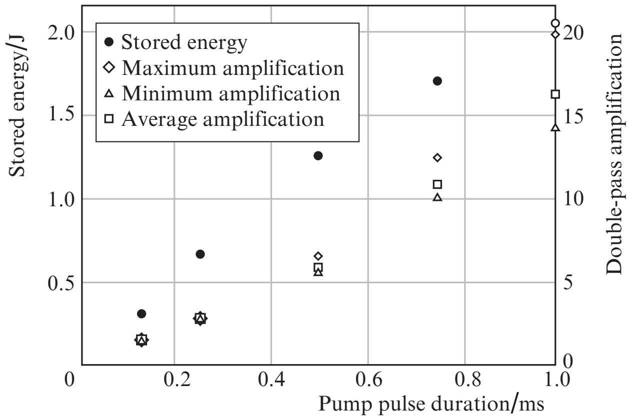

Figure 10. Dependences of the extracted energy and the gain in the laser head on the duration of the pump pulse for its constant peak power (4 kW).

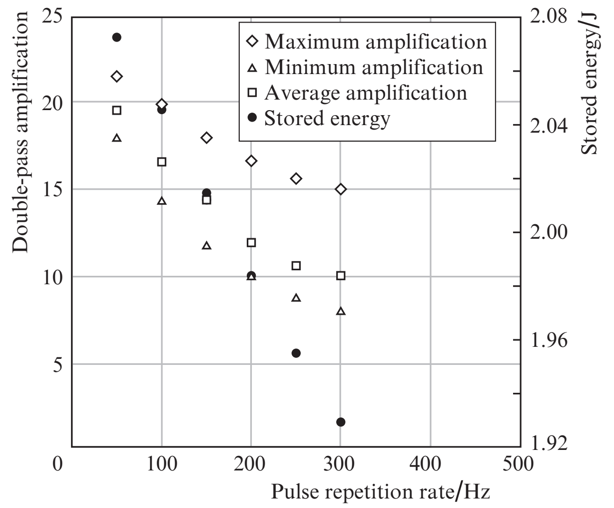

Figure 11. Gain and stored energy in relation to the pump pulse repetition rate. The pulse duration is 1 ms, the energy is 4 J.

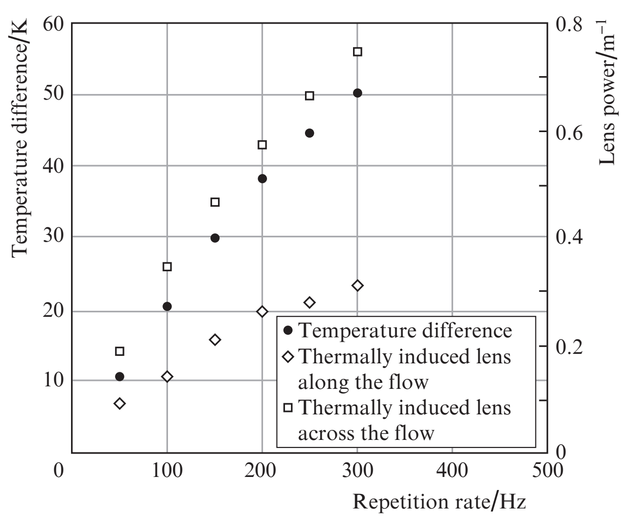

Figure 12. Dependences of the temperature difference and the thermal lens power on the pump pulse repetition rate. The pulse duration is 1 ms, the energy is 4 J.

a laser operating with pump pulses with an energy up to 4 J and a repetition rate up to 300 Hz. The simulation of cooling regimes, temperature distribution, and population inversion in the active zone was carried out. It is shown that the use of disks makes it possible to provide efficient cooling and an acceptable level of radiation losses and phase distortions at a pulse repetition rate of 100 Hz. A significant improvement in performance by significantly lowering the refrigerant temperature has also been demonstrated. When the coolant temperature changes from 293 to 193 K, the calculated small-signal gain for two passes through the active zone increases from 3- to 15-fold, and the stored energy increases from 1.5 to 2 J. A significant increase in the gain is mainly due to an increase in the gain cross section in Yb: YAG upon cooling. In this case, the beam quality parameter M^2 is 2.5 at room temperature of the coolant and 1.86 at cryogenic temperature. These results demonstrate the significant advantages of combining liquid cooling of a solid-state active medium with cryogenic cooling.

The proposed concept is optimal for amplification of pulses with a joule energy level in combination with a high pulse repetition rate and can be a good alternative to amplifiers based on cryogenically cooled 'active mirrors' or similar multi-disk heads with cryogenic cooling by helium flow. In the future, it is planned to experimentally test the proposed concept of the amplifying element.

Acknowledgements. The work was supported by the World-Class Research Centre "Photonics Centre" under the financial support of the Ministry of Science and High Education of the Russian Federation (Agreement No. 075-15-2020-906).

References

1. Banerjee S., Ertel K., Mason P.D., Phillips P.J., De Vido M., Smith J.M., Butcher T.J., Hernandez-Gomez C., Greenhalgh R.J.S., Collier J.L. *Opt. Express*, **23**, 15 (2015).
2. Siebold M., Loeser M., Harzendorf G., Nehring H., Tsybin I., Roeser F., Albach D., Schramm U. *Opt. Lett.*, **39**, 12 (2014).
3. Sawicka M., Divoky M., Novak J., Lucianetti A., Rus B., Mocek T. *J. Opt. Soc. Am. B*, **29**, 6 (2012).
4. Yasuhara R., Kawashima T., Sekine T., Kurita T., Ikegawa T., Matsumoto O., Miyamoto M., Kan H., Yoshida H., Kawanaka J., Nakatsuka M., Miyanaga N., Izawa Y., Kanabe T. *Opt. Lett.*, **33**, 15 (2008).
5. Fu X., Liu Q., Yan X., Cui J. *Chin. Opt. Lett.*, **7**, 492 (2009). DOI: 10.3788/col20090706.0492.
6. Goodno G.D., Palese S., Harkenrider J., Injeyan H. *Opt. Lett.*, **26**, 21 (2001).
7. Brown D.C., Cone R.L., Sun Y., Equall R.W. *IEEE J. Sel. Top. Quantum Electron.*, **11**, 3 (2005).
8. https://www.lauda.de/ru/termostatirujushchee-oborudovanie/termostaty/okhlazhdajushchie-termostaty/pro/product/PRO-RP-10100.
9. https://loip.ru/catalog/laboratornoe-oborudovanie-proizvodstva-loip/laboratornye-termostaty-i-kriostaty/nizkotemperaturnyie-termostatyi-serii-loip-ft/loip-ft-311-80.
10. Fan T.Y. *IEEE J. Quantum Electron.*, **29**, 6 (1993).
11. Stabnikov V.N., Roiter I.M., Protsyuk T.B. *Etilovyi Spirt* (Ethyl Alcohol) (Moscow: Pishchevaya Promyshlennost', 1976).
12. Sergacheva E.V. Cand. Diss. (St. Petersburg, SPbGETU, 2018).
13. Baron N.M., Ponomareva A.M., Ravdel' A.A., Timofeeva Z.N. *Kratkii Spravochnik Fiziko-Khimicheskikh Velichin* (A Short Handbook of Physical and Chemical Quantities) (St. Petersburg: Ivan Fedorov Publ., 2003).
14. Casagrande O., Deguil-Robin N., Garrec B.L., Bourdet G.L. *IEEE J. Quantum Electron.*, **43**, 2 (2007).